

REDUCTION OF ECA AMOUNT FOR THE RIBBON INTERCONNECTION OF HETEROJUNCTION SOLAR CELLS

Christina Kaiser, Veronika Nikitina, Torsten Geipel, Achim Kraft
 Fraunhofer Institute for Solar Energy Systems (ISE)
 Heidenhofstr. 2, 79110 Freiburg, Germany, christina.kaiser@ise.fraunhofer.de

ABSTRACT: Electrically conductive adhesives (ECAs) offer a low temperature alternative for the ribbon interconnection of temperature sensitive silicon heterojunction (SHJ) solar cells. The main drawbacks of ECAs are their high costs. To overcome this problem the used ECA amount is reduced by changing the application pattern. Four different patterns are investigated in terms of ECA reduction and long-term stability in TC200. Two different ECAs are analyzed in terms of DSC, TGA, electrical properties and rheology and 1-cell-strings with the four patterns for each ECA are produced for peel test analysis. One of the ECAs is used for the production of 3-cell-modules in glass-backsheet configuration with each of the application patterns to analyze module performance via I-V-measurements and EL imaging. In addition, the modules are aged via TC200. For lower ECA amounts a slightly higher degradation is observed but relative losses in FF are below 5 %.

Keywords: electrically conductive adhesive, cost reduction, heterojunction, module, PV materials, ribbon interconnection, contact

1 INTRODUCTION

Silicon heterojunction (SHJ) solar cells based on amorphous silicon thin films and crystalline silicon wafers with front and rear metallization achieve conversion efficiencies up to 24% on industrial scale [6]. As amorphous silicon layers show severe degradation when exposed to temperatures > 220 °C for longer durations, metallization and interconnection of SHJ solar cells require particular attention during fabrication. The metallization of SHJ solar cells is realized with low temperature metallization pastes. One of the main drawbacks of these metallization pastes is the weak adhesion to the wafer, which makes the cell interconnection process by soldering very challenging [1, 2]. One possibility to overcome this problem is to use electrically conductive adhesives (ECAs) for the ribbon interconnection [5]. In addition, ECAs are cured at a low temperature (typically between 130 °C and 180 °C), which reduces the risk of damaging the sensitive SHJ solar cells during the interconnection process.

ECAs are composites based on a polymeric matrix filled with electrically conductive particles. Typical matrix materials are epoxies, acrylates or silicones which are cured by heat [8]. For filler materials different metallic particles, mostly silver flakes or spheres are used but also metal coated polymers or glass particles can be used. To ensure a good conductivity the filler content is between 25 and 30% vol [7].

The key challenge for the ECA interconnection technology of SHJ solar cells is the reduction of costs while maintaining efficiency and long-term stability of photovoltaic (PV) modules [4]. This paper describes the experimental route for ECA reduction by variation of the screen printing application pattern, while taking into account material properties of two different ECAs.

2 MATERIAL AND METHODS

In order to reduce ECA consumption in the interconnection process the screen design is varied. Four different screens with a variation of the printing pattern are used for the application of two ECAs on the front (f) and rear (r) side of industrial busbar-less SHJ solar cells.

Fig. 1 shows a schematic of the printing patterns. Patterns A and B are continuous patterns, which do not change along the cell length. Pattern C and D have, so called, pad areas at the edges of the cell and in the center the ECA is applied in form of small rectangles (“dotted” area).

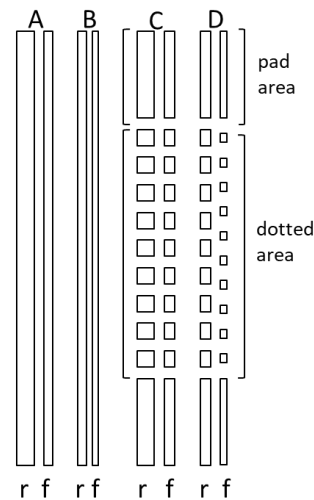


Figure 1: Schematic of the screen design of the screens (A, B, C, D), with pattern applied to rear (r) and front (f) side of the solar cell. Geometries are not drawn to scale.

For the experiments two commercially available ECAs (ECA I and ECA II) are chosen based on industrial relevance. They are both filled with silver particles. The ECAs are characterized in terms of differential scanning calorimetry (DSC) measurements, electrical resistivity, thermogravimetric analysis (TGA) and rheology.

DSC measurements are conducted with about 10 mg ECA and a constant heating rate of 10 K/min from 30 °C to 200 °C. They are run at least twice to ensure complete curing. TGA was performed on cured samples of about 30 mg ECA from room temperature up to 600 °C and kept at that temperature for at least four hours.

The volume resistivity of both ECAs was measured according to MIL-STD-883H and the joint resistance was measured with the transfer line method (TLM) for joints between two Ag-coated copper ribbons. Both methods

are four-point measurement methods. For the TLM measurements the ECA was applied by dispensing a small dot onto a ribbon (Ag-coated copper ribbon, with a cross section of 1.0 mm x 0.2 mm) and placing a second ribbon onto the dot, thus creating a joint with an area smaller than 1 mm².

The rheological behavior of the two ECAs was measured with a rotational rheometer at 25 °C with a plate-plate geometry at increasing shear rates between 0.01 and 20,000 s⁻¹. The measurement was repeated three times for each ECA.

The industrial n-type bifacial silicon heterojunction (SHJ) solar cells used for string production are supplied by an external partner. They feature five pairs of fingers instead of five regular busbars.

Individually connected cells and 3-cell-strings are automatically produced on a TT1600 ECA-stringer by teamtechnik GmbH. Here, the ECA is applied by screen printing and curing is done with hot plates at a temperature of 195 °C for about 30 s for both ECAs. The ribbons used for solar cell interconnection are copper ribbons with an Ag-coating which have a cross section of 1.0 mm x 0.2 mm. In addition, they possess a light-reflective structure on one side.

Before and after the application of ECA, the cells are weighed in order to determine the amount of ECA. To support the selection of an optimal screen design the measured application amounts are compared to theoretical calculations.

As peel strength of the interconnection plays a significant role during the module manufacturing process 90° peel tests at a speed of 50 mm/min are performed for all printing patterns on the connected cells. The measured force is normalized to the ribbon width.

For the determination of the influence of ECA amount and printing pattern on the module performance, current-voltage (*I-V*) measurements and electroluminescence (EL) imaging was performed on 3-cell-modules with ECA I. Three glass-backsheet modules are produced for each application pattern. The encapsulation material is a thermoplastic polyolefin (TPO) with UV blocking properties. A solar-grade glass with a thickness of 3.2 mm is used and a PET-based backsheet with an additional water diffusion barrier.

Thermal cycling according to IEC 61215 [3] is performed on the modules for 200 cycles. *I-V* measurements and EL imaging was conducted before and after aging.

3 RESULTS AND DISCUSSION

3.1 ECA Characterization

DSC analysis shows a curing reaction of ECA I that starts at about 59 °C and at about 66 °C for ECA II (see Fig. 2).

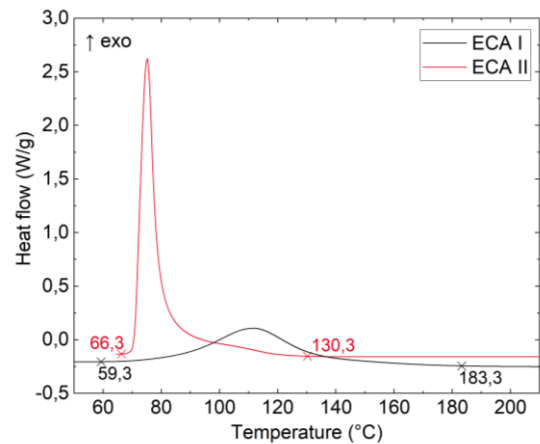


Figure 2: DSC analysis of ECA I and ECA II. Start and end temperature of curing reaction are shown.

The volume resistivity of ECA II was $12 \pm 4 \times 10^{-3} \Omega\text{cm}$ and the joint resistance was $0.9 \pm 0.6 \text{ m}\Omega$. For ECA I the volume resistivity was too high to be measured with the instrumentation available for this experiment, but a joint resistance of $0.3 \pm 0.3 \text{ m}\Omega$ could be measured. This shows that ECA I has anisotropic characteristics rather than isotropic, which is not surprising as it has a reduced silver content according to the manufacturer.

The joint resistance was measured for a joint between two Ag-coated ribbons. Therefore, it does not represent the exact resistance of an ECA joint in a PV module, which is between the grid fingers and the ribbon surface. The high error values might be explained by variations in the joint geometries and inhomogeneities of the filler distribution in the ECA. In addition, the mechanical stability of the joints is low due to the very small joint areas. This might influence the joint resistance measurements as well, since an electrical contact can only be constant if a mechanical contact is given.

Thermogravimetric analysis of cured samples shows a mass loss of 47% for ECA I and 41% for ECA II, which contributes to the observations of electrical anisotropy for ECA I. An assumption about the actual filler content for the ECAs should be avoided as TGA was performed under a nitrogen atmosphere and residual ash content from the organic matrix might contribute to the remaining mass.

Another indication of lower filler content in ECA I is its lower viscosity at shear rates between 0.01 and 100 s⁻¹ compared to ECA II, which shows a significant higher viscosity (see Fig. 3).

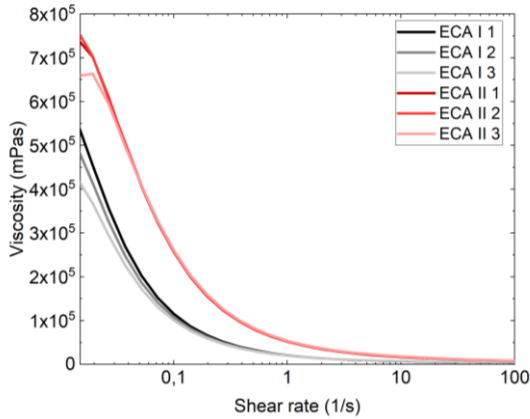


Figure 3: Viscosity of ECA I and ECA II vs. shear rate measured at 25 °C and repeated for three samples each.

3.2 ECA Amount

The applied amount of ECA was reduced by nearly 50% for both ECAs. In total, a reduction from 81 mg to 44 mg per cell was reached for ECA I and a reduction from 102 mg to 54 mg per cell was reached for ECA II (see Fig. 4).

For the calculation of the ECA amount applied to a solar cell with a given screen design the area of the open screen pattern is calculated. Furthermore, the theoretical color volume of the screen fabric is considered to calculate the volume of the ECA applied to the cell. The theoretical color volume is a value which takes into account the screen characteristics, such as wire diameter and wire number. By multiplying this volume with the area of the screen pattern and the density of the ECA, taken from the ECA datasheet, a theoretical mass of ECA per cell (m_{ECA}) can be calculated:

$$m_{\text{ECA}} = A_{\text{screen}} \cdot V_{\text{th}} \cdot \rho_{\text{ECA}} \quad (1)$$

A_{screen} is the area of the screen pattern, V_{th} the theoretical color volume and ρ_{ECA} the density of the ECA.

The theoretical color volume is calculated as follows:

$$V_{\text{th}} = \frac{\alpha_0 \cdot D}{100} \quad (2)$$

with fabric thickness D and percentage of open area α_0 [8].

The percentage of open area is calculated from the mean value of mesh-openings and the actual thickness of the threads (d):

$$\alpha_0 = \frac{w^2 \cdot 100}{(w + d)^2} \quad (3) \quad d = \frac{10000}{n} - w \quad (4)$$

The mesh opening w is the distance between two contiguous warp or weft threads and n is the mesh count which is given by the number of threads per centimeter [8].

The calculated results are compared to results obtained through weighing (Fig. 4).

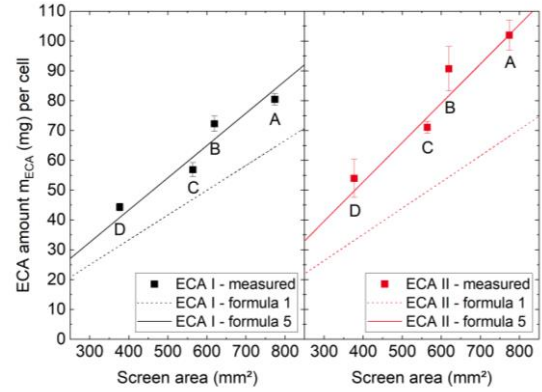


Figure 4: Summary of ECA amounts measured by weighing of solar cells before and after ECA application with standard deviation as error bars and by calculation with formula (1) (dotted line) and formula (5) (full line).

The calculated values for the ECA amount do not completely comply with the measured values. The theoretical color volume underestimates the real amount. It is not sufficient to predict the actual amount applied. The color volume is only an approximate value for the applied volume with a specific screen. In addition, it is a value for printing inks and not for ECAs.

The difference of the applied amount between the two ECAs can be partly explained by the different densities. However, the higher difference between calculated and measured amount for ECA II in comparison to ECA I shows that another factor influences the value as well. Additional analysis of cross-sections of the joints shows that the joint thickness for ECA II is higher than for ECA I. This might be due to a higher viscosity of ECA II. An influence of the screen printing parameters can be eliminated as the same parameters were used for both ECAs during the application.

To overcome the high differences between calculated and measured amount a correction factor c can be used:

$$m_{\text{ECA}} = A_{\text{screen}} \cdot V_{\text{th}} \cdot \rho_{\text{ECA}} \cdot c \quad (5)$$

There is not one correction factor for every ECA but it has to be determined for each ECA separately. For ECA I a correction factor of 1.3 shows a good agreement with the measured values. For ECA II this is 1.5 (see Fig. 4). Nevertheless, these factors are only preliminary estimates and further experiments are necessary to verify the values.

The model to describe the applied amount has to be further improved. Amongst others, following parameters influence the printing: the velocity of the squeegee, the shore hardness of the squeegee, its adjustment angle and its edge shape. For example a low velocity, low hardness and pressure of the squeegee lead to higher application amounts. In addition, the consistency of the material applied and the roughness of the surface, to which the material is applied to, play a significant role in the amount applied. A high surface roughness, as given by the textured surface of a solar cell, leads to a higher application of printed material [9].

3.3 Peel Tests

Peel tests are performed on front and rear side of the cells for both ECAs and each screen. The peel forces

correlate with the printing pattern on the dotted screen. At the continuous areas, the peel forces are higher and they are lower at areas with a dotted pattern (see Fig. 5). Therefore, the peel forces are analyzed separately for areas with pads and areas with a dotted pattern. This can be observed for both ECAs.

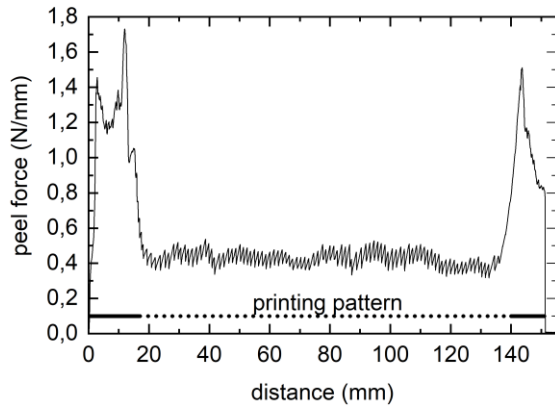


Figure 5: Results of a peel test for printing pattern D (schematic representation of the printing pattern in the graph) at the front side of a solar cell with ECA I.

Fig. 6 shows a summary of the peel forces of both ECAs and every printing pattern. ECA I shows peel forces higher than 1 N/mm for continuous printing patterns A and B, as well as for the pad areas of printing patterns C and D. The peel forces at the dotted areas are between 0.3 and 0.7 N/mm, dependent on cell side and screen. Since the highest stresses on the ribbon interconnection of solar cells occur at the edges of the solar cell, the high peel strength at the edges should be sufficient to ensure a reliable interconnection.

ECA II shows overall lower peel forces than ECA I. Even for continuous printing patterns, the values do not reach 1 N/mm.

The peel strength is determined with the assumption that the adhesive width equals the width of the ribbon (in this case 1 mm). However, a microscopic analysis of the area shows that the real adhesion width is lower than one millimeter in most cases. Therefore, the real peel forces per millimeter adhesion width should be greater for both ECAs and especially at the front sides and for the printing patterns with low application widths.

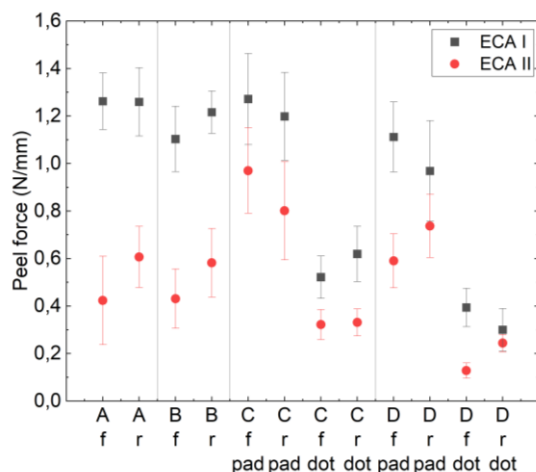


Figure 6: Summary of the peel forces on front side (f) and rear side (r) for all printing patterns. For pattern C and D individual analysis for pad and dotted (dot) areas are shown. Error bars show the standard deviation.

3.4 I-V and EL Characterization

I-V measurements of ECA I on glass-backsheet modules do not show any significant differences between the modules with different application patterns as a measurement uncertainty of 1% has to be considered. Fig. 7 shows the fill factor (FF) and the power at maximum power point (P_{MPP}) for all the 3-cell-modules produced with ECA I. The absolute cell-to-module loss of FF for ECA I is in the range of 1.7% to 1.9%, the cell-to-module losses in P_{MPP} are about 0.25 W. EL imaging shows no special conspicuous features for any of the modules.

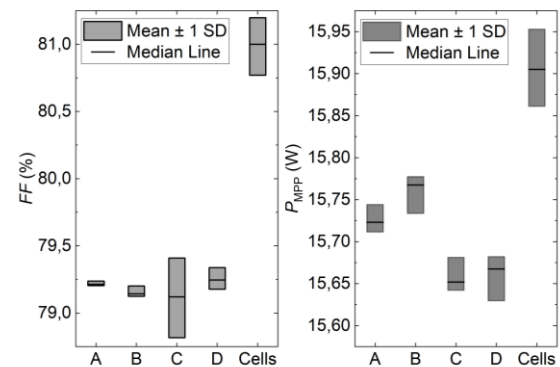


Figure 7: Box plot of FF and P_{MPP} of the 3-cell-modules in glass-backsheet configuration of ECA I for all printing patterns and the FF and P_{MPP} of the cells used for module production.

3.5 TC200

I-V measurements show a higher loss in P_{MPP} and FF for printing patterns C and D compared to printing patterns A and B (Fig.8). Nevertheless, the loss is below 5% for all modules except module C3. The probable cause of failure in this module might be a partial detaching of the cross-connector and therefore should be taken into account with caution when interpreting losses due to ECA amounts. A measurement uncertainty of 1% has to be taken into account when interpreting the changes in terms of ECA failure, as well.

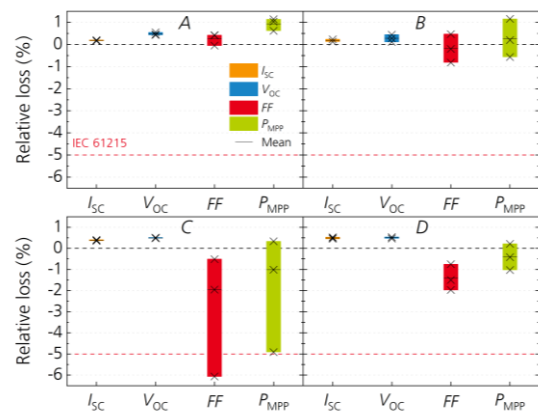


Figure 8: Relative losses in I_{sc} , V_{oc} , P_{MPP} and FF of the 3-cell-modules in glass-backsheet configuration of ECA I for all printing patterns (A, B, C, D) after TC200. The values for the single modules are shown as x marks.

EL imaging shows that the degradation takes mostly place in the dotted areas of the ECA application (see Fig. 9, D after TC). This implies a degradation of the modules due to local failures in the ECA interconnection.

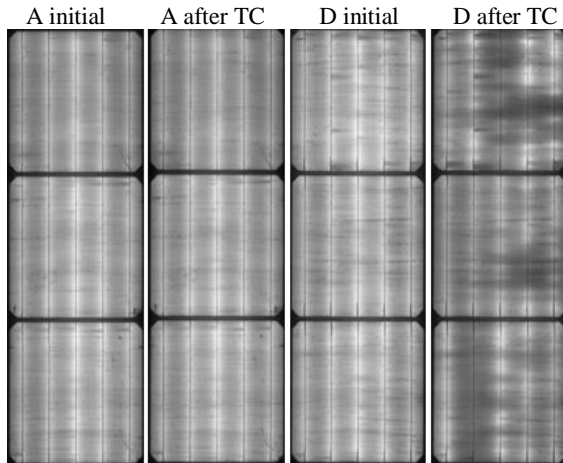


Figure 9: EL images of 3-cell-modules with application pattern A and D before and after TC200.

Nevertheless, the losses in module performance due to ECA interconnection failures might not be the only reasons for performance losses. Further investigation is necessary to determine the failure mechanisms and other sources for the losses. In addition, it might be possible to reduce losses by changing the bill of material for the modules. For example, by changing the encapsulation material and using a glass-glass configuration instead of a glass-backsheet configuration. In addition, another ECA might show less influence on module degradation due to the application pattern.

4 CONCLUSION

A reduction of ECA amount for the ribbon interconnection of SHJ solar cells was performed by variation of the printing pattern. The amount applied was measured and a model to estimate the amount was applied. In addition the ECAs used were characterized in terms of DSC analysis, TGA and rheological properties. 3-cell-modules in glass-backsheet configuration with ECA I were characterized in terms of IV measurements and EL imaging before and after TC200.

Following results were achieved:

- Reduction of ECA amount by about 50% without significant influence on electrical properties of modules.
- Rheological properties of an ECA influences the amount applied to a solar cell during screen printing.
- Electrical characterization and TGA measurement suggest anisotropic properties of ECA II due to a lower filler content.
- A linear correlation between calculated ECA amount and real ECA amount applied to a solar cell via screen printing was shown.
- The peel strength of ribbon interconnection is dependent on the ECA used and the application pattern.

- The peel strength is up to 1.3 N/mm for ECA I in continuously printed areas
- The application pattern and the amount applied show no significant influence on cell-to-module losses concerning the fill factor.
- A lower ECA amount leads to higher losses in P_{MPP} and FF after TC200 using a glass-backsheet configuration with TPO encapsulant, but losses are below 5%.

7 REFERENCES

- [1] De Rose, A., Geipel, T., Erath, D., Kraft, A., and Eitner, U. 2018. Challenges for the interconnection of crystalline silicon heterojunction solar cells. *Photovoltaics International* 40, 78–86.
- [2] De Rose, A., Geipel, T., Eberlein, D., Kraft, A., and Nowotnick, M. Interconnection of silicon heterojunction solar cells by infrared soldering. solder joint analysis and temperature study. In *EU PVSEC 2019*.
- [3] DIN Deutsches Institut für Normung e. V. und VDE Verband der Elektrotechnik Elektronik Informationstechnik e. V., “Terrestrische kristalline Silizium-Photovoltaik-(PV-) Module Bauart-eignung und Bauartzulassung (IEC 61215:2005): Deutsche Fassung EN 61215:2005,” 2005, DIN EN 61215:2005.
- [4] Geipel, T. 2017. *Electrically Conductive Adhesives for Photovoltaic Modules*. Dissertation, Gottfried Wilhelm Leibniz Universität Hannover.
- [5] Geipel, T., Nikitina, V., Bauermann, L. P., Fokuhl, E., Schnabel, E., Erath, D., Krieg, A., Kraft, A., Fischer, T., Lorenz, R., and Breitenbücher, D. Industrialization of Ribbon Interconnection for Silicon Heterojunction Solar Cells with Electrically Conductive Adhesives. In *EU PVSEC 2019*.
- [6] Haschke, J., Dupré, O., Boccard, M., and Ballif, C. 2018. Silicon heterojunction solar cells. Recent technological development and practical aspects - from lab to industry. *Sol Energ Mat Sol C* 187, 140–153.
- [7] Lewis, H. J. and Coughlan, F. M. 2008. An overview of the use of electrically conductive adhesives (ECAs) as a solder replacement. *Journal of Adhesion Science and Technology* 22, 8-9, 801–813.
- [7] Pujol, J. M., Prud'homme, C., Quenneson, M. E., and Cassat, R. 1989. Electroconductive Adhesives: Comparison of Three Different Polymer Matrices. Epoxy, Polyimide and Silicone. *The J. of Adhesion* 27, 4, 213–229.
- [9] Sefar AG Division Druck. 2007. *Siebdruckhandbuch. Vorsprung durch Wissen*, Thal Schweiz.